11th International Symposium on Turbulence and Shear Flow Phenomena (TSFP11)
Southampton, UK, July 30 to August 2, 2019

A SURFACE-MOUNTED BLUFF BODY IN HIGHLY PULSATILE FLOW: EFFECTS OF FREESTREAM INFLOW FREQUENCY

Ian Carr
Department of Mechanical and Aerospace Engineering
The George Washington University
800 22nd St. NW Washington, DC, USA 20052
icarr@gwu.edu

Nikolaos Beratlis
School for Engineering of Matter, Transport and Energy
Arizona State University
P.O. Box 879309, Tempe, AZ, USA 85287
nikos.beratlis@gmail.com

Elias Balaras
Department of Mechanical and Aerospace Engineering
The George Washington University
balaras@gwu.edu

Michael W. Plesniak
Department of Mechanical and Aerospace Engineering
The George Washington University
plesniak@gwu.edu

ABSTRACT

Bluff body wake dynamics have been a persistent focus of study due to their sensitivity to small parameter changes. The introduction of large amplitude freestream pulsatility has proven, in our prior studies, to provide insight into bluff body wakes in general. In this study we focus on the effect of the frequency of the large-scale freestream fluctuations, ranging from vortex lock-in frequencies on the high end to quasi-steady wake configurations on the low end. A series of direct numerical simulations, validated against previous experiments, were performed at several values of reduced frequency. A selection of representative cases through the a broad range of reduced frequency are presented. Contours of Q-criterion and velocity fields in the near wake and freestream elucidate the evolution of the wake with increasing reduced frequency of freestream pulsatility. From these data a regime map for flows of this type was developed.

INTRODUCTION & BACKGROUND

Biological and biomedical flows often fall into a category of flows referred to as "pulsatile flows". Pulsatile flows are those with cyclic fluctuations, typically due to an imposed forcing, superimposed on a mean flow. Cardiovascular flows, i.e. those originating from a beating heart, are the most well-studied highly pulsatile flows. A large portion of that study is focused on developing understanding with simplified models of more complex systems, i.e. curved pipes of varying radii and curvature, simplified bifurcation configurations, etc. In contrast, unbounded flow around obstacles, a canonical and widely applicable configuration, exposed to highly pulsatile flow has received very little study. As biomedical device design and the study of biological fluid dynamics advances the need for fundamental understanding will only increase. This study contributes to that knowledge base and provides a useful reference for researchers studying complex pulsatile flows.

In this study we computationally investigate the wake of surface-mounted hemisphere under highly pulsatile flow conditions and vary the frequency of the flow pulsatility. We define highly pulsatile flow as flow in which the velocity fluctuations are cyclic and of the same magnitude as the mean velocity. Highly pulsatile flow spans a wide parameter space in which the amplitude, frequency, mean velocity, and inflow profile shape can all be varied. Holding all other parameters constant we vary the frequency of freestream flow pulsatility ranging from a low-frequency, quasi-steady regime to a high-frequency pulsatility on the order of the natural vortex shedding that occurs in steady flow of the same Reynolds number (Re).

The parameter of interest is the reduced frequency, k, defined as,

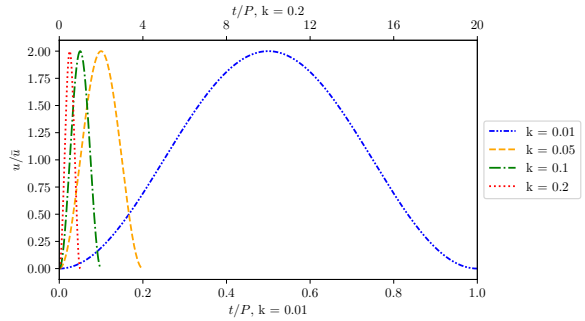

Figure 1. The range of inflow profiles studied. The sinusoidal profiles served as the inlet condition for the corresponding simulation ranging from $k = 0.01$ to $k = 0.2$.

$$k = \frac{Rf}{\bar{u}} = \frac{R}{\bar{u}P}, \tag{1}$$

where R is the hemisphere radius, f is the frequency of the pulsatility, $\bar{u}$ is the average streamwise velocity, and P is the period. The value of k is varied holding all other parameters constant. The inflow waveforms examined herein are shown in figure 1. The inflow velocity, u, is normalized by the mean velocity of the cycle, $\bar{u}$, and time, t, is normalized by the duration of one period, P. The range of frequencies was chosen to span from near steady freestream flow to freestream pulsatility near the frequency of natural vortex shedding in flows of this type. The range of Reynolds number was chosen to be relevant to physiological and biological applications, i.e. on the order of 1000.

The literature which informed this study is broad and spans several areas of study within fluid dynamics. Ranging from the study of the flow around a variety of surface-mounted obstacles to vortex ring propagation to impulsively started flows and starting vortices, fully contextualizing this work is out of the scope of this manuscript. Fig. 2 depicts the wake structure schematics essential for understanding the present study. Acarlar & Smith (1987) was an early, seminal work which, among other studies, established the vortex topology for surface-mounted hemisphere in *steady* freestream flow. The essential wake structures, depicted in Fig. 2(a), are the hairpin vortices cyclically shed from the shear layer in the near wake. Carr & Plesniak (2016) established the phase-averaged wake topology in *pulsatile* flow, depicted in Fig. 2(b). The primary, phase-averaged structure is an arch-type vortex which forms during accelerating inflow and propagates upstream during decelerating inflow. Detailed analysis and characterization can be found in the full manuscript (Carr & Plesniak, 2016). The objective of the present study is to understand the dependence of pulsatile frequency on the arch-type vortex through numerical simulation.

NUMERICAL METHODS

The pulsatile simulations were carried out using an in-house finite difference Navier-Stokes code, wherein the governing equations for a viscous incompressible flow were discretized on a structured grid in Cartesian space. The geometry of the hemisphere, which was not aligned with

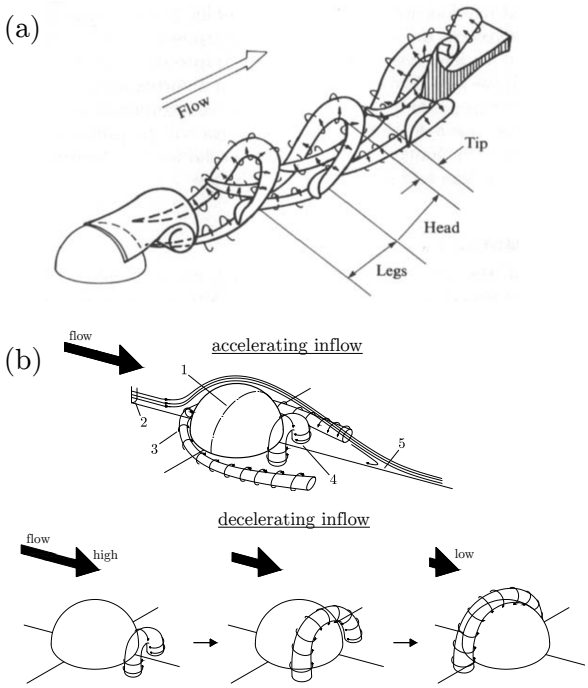

Figure 2. (a) A schematic representation of the vortex structures in the wake of a surface-mounted hemisphere in steady freestream flow from (Acarlar & Smith, 1987). (b) A schematic representation of the phase-averaged vortex structures in the wake of a surface-mounted hemisphere in highly pulsatile freestream flow (Carr & Plesniak, 2016).

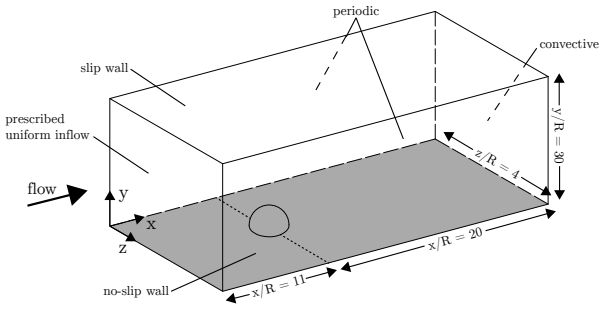

Figure 3. Simulation domain with prescribed boundary conditions. Not to scale.

the grid, was treated using an immersed-boundary formulation. An exact, semi-implicit projection method was used for time advancement. All terms were treated explicitly using a Runge-Kutta 3rd order scheme with the exception of the viscous and convective terms in the wall-normal direction. Those terms were treated implicitly using a 2nd order Crank-Nicholson scheme. All spatial derivatives were discretized using a 2nd order, central-difference scheme on a staggered grid. The code is parallelized using a classical domain decomposition approach. The domain was evenly divided in the streamwise direction and communication between the processed is handed with MPI library calls. The inlet boundary condition was a uniform pulsatile velocity matched with the experiments. The simulations were computed on George Washington University's Colonial One Cluster and used 50 CPU cores. More details of the solver can be found in Beratlis *et al.* (2007).

The computational domain, shown in Fig. 3, measures 31R x 30R x 4R in the streamwise, wall normal, and spanwise directions, respectively. The hemisphere is centered at the origin. The inlet and the outlet are located 11R upstream and 20R and downstream of the hemisphere. The boundary conditions are no-slip wall at the bottom, slip wall at the top, and periodicity in the spanwise direction. At the outlet a convective boundary condition is used while at the inlet a pulsatile uniform velocity profile is prescribed. The grid contains 650 x 280 x 200 points in the x, y and z directions respectively. Near the surface of the hemisphere the grid resolution is $D_x = 0.01R$, $D_y = 0.01R$ and $D_z = 0.02R$. The grid resolution is sufficient to capture all the important flow structures and is in agreement with with the experiments. The simulations were initialized with uniform flow and time probes were placed in the flow to monitor the evolution of the transient state. It was found that after approximately $100R/U$ time units the flow reached a periodic state.

Plotting and visualization of the results was performed in ParaView 5.5.0. In-plane velocity vectors are composed of only the in-plane components of velocity. Derived quantities, such as vorticity and vortex identification methods, were calculated during post processing. The primary vortex identification method used is Q-criterion, which is defined as a connected region with a positive second invariant of the velocity gradient tensor (Hunt *et al.*, 1988).

RESULTS

A representative selection of the simulated values of k are presented below. The flow field will be represented by a plane of velocity and Q-criterion contour. The plane is oriented in the streamwise direction, normal to the base plane and bisects the obstacle at its midpoint ($z/D = 0$). The arrows indicate only flow direction and are not scaled by velocity magnitude as to represent the entire flow field despite its large dynamic range. If scaled with velocity magnitude the structure of the near wake would not be visually parsable. For each value of k four phases will represent the entire pulsatile cycle. In Fig. 1, minimum velocity corresponds to $t/P = 0.0$ and maximum velocity corresponds to $t/P = 0.5$. For clarity, the phases labelled 50% accelerating and 50% decelerating refer to 50% through the accelerating and decelerating portion of the inflow waveform, respectively, ($t/P = 0.0$ to 0.5 for accelerating), not 50% of the rate of change of velocity.

Starting with $k = 0.01$, Fig. 4, the wake of the hemisphere largely represents a set of quasi-steady flow fields. The structure of the wake is composed of the same essential features as are present in steady flow and represented in Fig. 2(a). There is some very low magnitude Q-criterion content remaining from the previous cycle in Fig. 4(a). Through accelerating inflow, maximum velocity, and decelerating inflow (Fig. 4(b,c,d)) the wake is composed of an area of intense mixing capped by a free shear layer. At the shear layer's downstream most extent in Fig. 4(c), signs of shear layer roll-up can be observed and are indicated by an arrow ($x/D = 1.5$, $y/D = 0.5$). This roll-up leads to the production of hairpin vortices as is typical in steady flow at this Re. Finally the shear layer begins to rise, moving away from the base plane as the flow decelerates.

In the $k = 0.05$ case, Fig. 5, the vortical content, as marked by Q-criterion, remaining from the previous cycle is visible throughout the field of view at minimum velocity (Fig. 5(a)). This remnant vortical content is convected

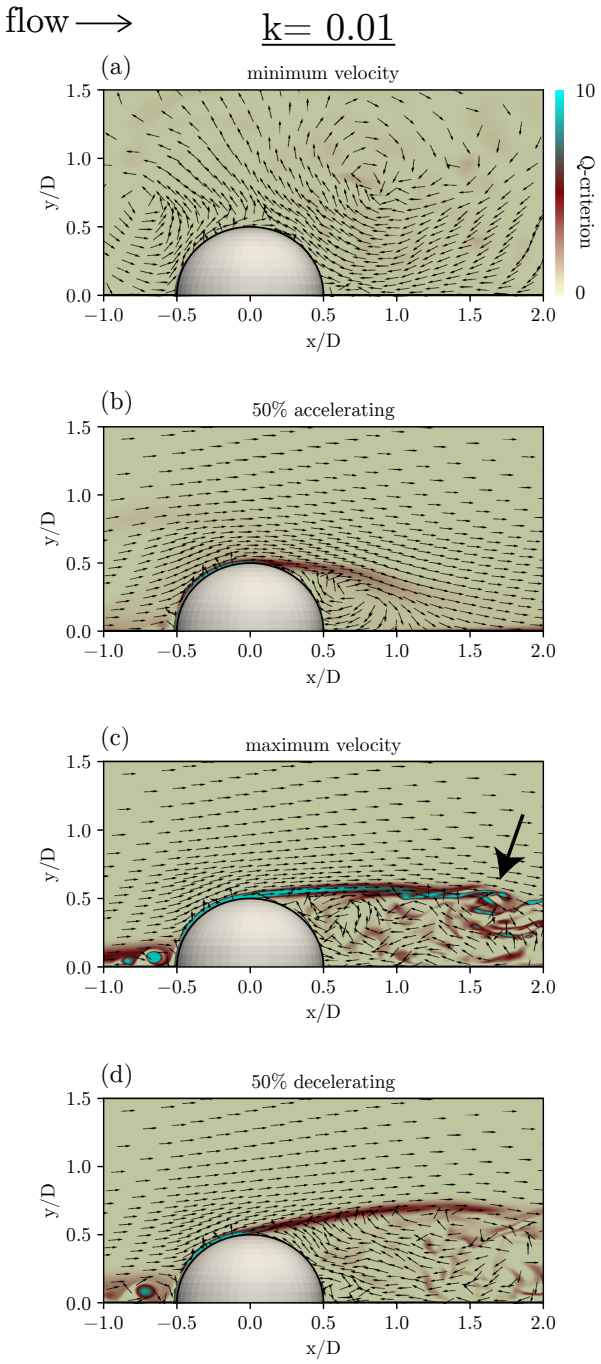

Figure 4. Velocity vector fields with Q-criterion contours around a surface-mounted hemisphere in highly pulsatile flow for the $k = 0.01$ case.

downstream through accelerating inflow. As the reduced frequency is increased five fold, there is considerably less time for the shear layer, and associated hairpin vortices, to develop. This reduced wake development is perhaps most clearly observed at maximum velocity (Fig. 5(c)). While the wake in previous case (Fig. 4(c)) is near indistinguishable from a wake in steady freestream flow, the increased reduced frequency restricts the growth of the shear layer and wake — only extending to $x/D \approx 1.3$ in Fig. 5(c). Finally during deceleration, the relative brevity of the decelerating phases means much of the vortical content persists through all of decelerating inflow and into the next cycle. While

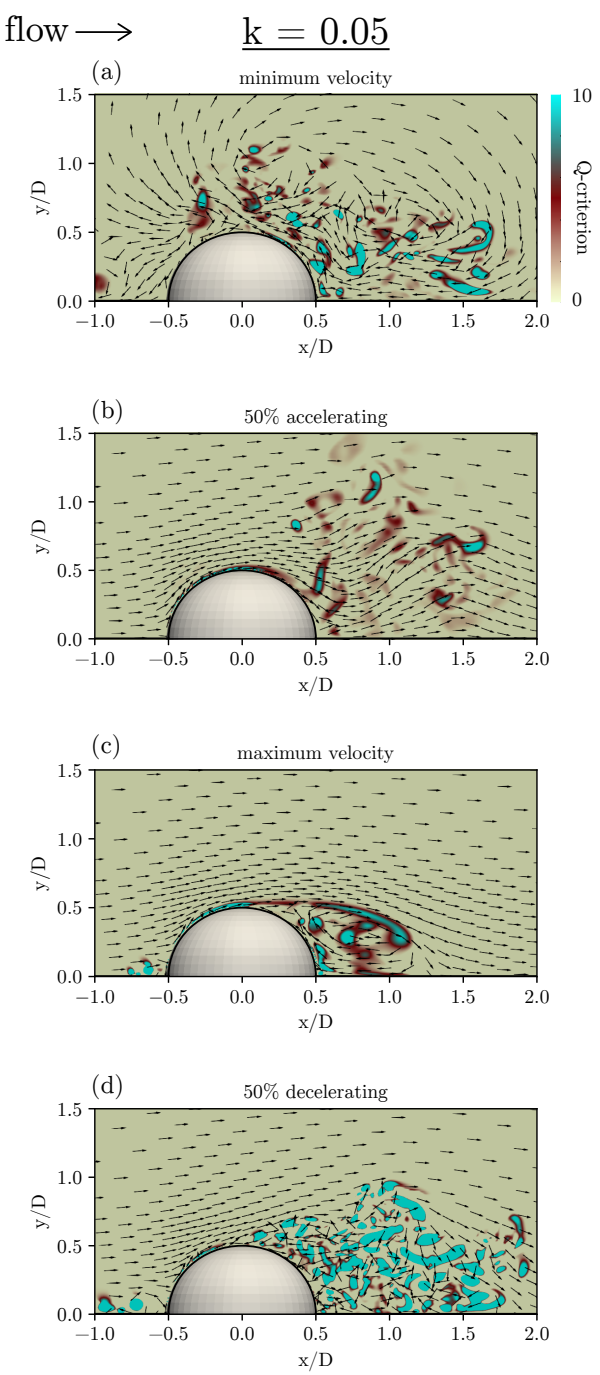

Figure 5. Velocity vector fields with Q-criterion contours around a surface-mounted hemisphere in highly pulsatile flow for the $k = 0.05$ case.

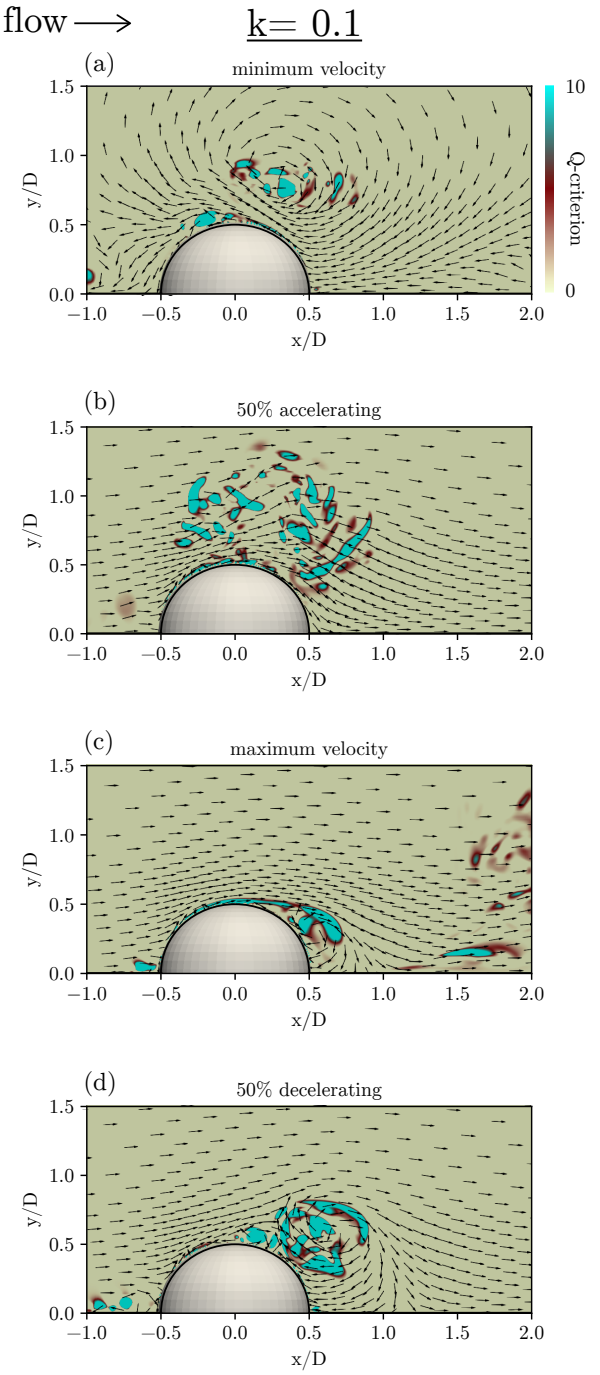

Figure 6. Velocity vector fields with Q-criterion contours around a surface-mounted hemisphere in highly pulsatile flow for the $k = 0.1$ case.

there is certainly no coherent arch-type vortex structure in this case, the organization of the near wake and recirculation region suggests some emerging organization.

In the next case the reduced frequency is doubled to $k = 0.1$. This is approaching the value of natural shedding frequency, equivalent to Strouhal number (St) = 0.2, in steady flow of the average Re (1000). As this value is approached the wake dynamics are expected to change significantly. At minimum velocity $k = 0.1$ (Fig. 6(a)), the vortical content and velocity field is relatively organized — containing a localized region of packets of Q-criterion surrounded by circular streamlines. Additionally, there is a small region of high Q-criterion near the surface of the hemisphere. During accelerating inflow (Fig. 6(b)), the remaining vortical content breaks up loosing what coherence it had. At maximum velocity (Fig. 6(c)), the near wake is organized and compact containing a packet of high Q-criterion surrounded by a circular vector field. This is arch shaped organization is the first clear evidence of the arch vortex in an instantaneous sense. Finally during decelerating inflow (Fig. 6(d)) the arch vortex loses coherence and breaks up as it lifts into the freestream. This is the first case in which the arch-type vortex begins to emerge — a ragged structure in this case.

At the highest reduced frequency, $k = 0.2$, the near

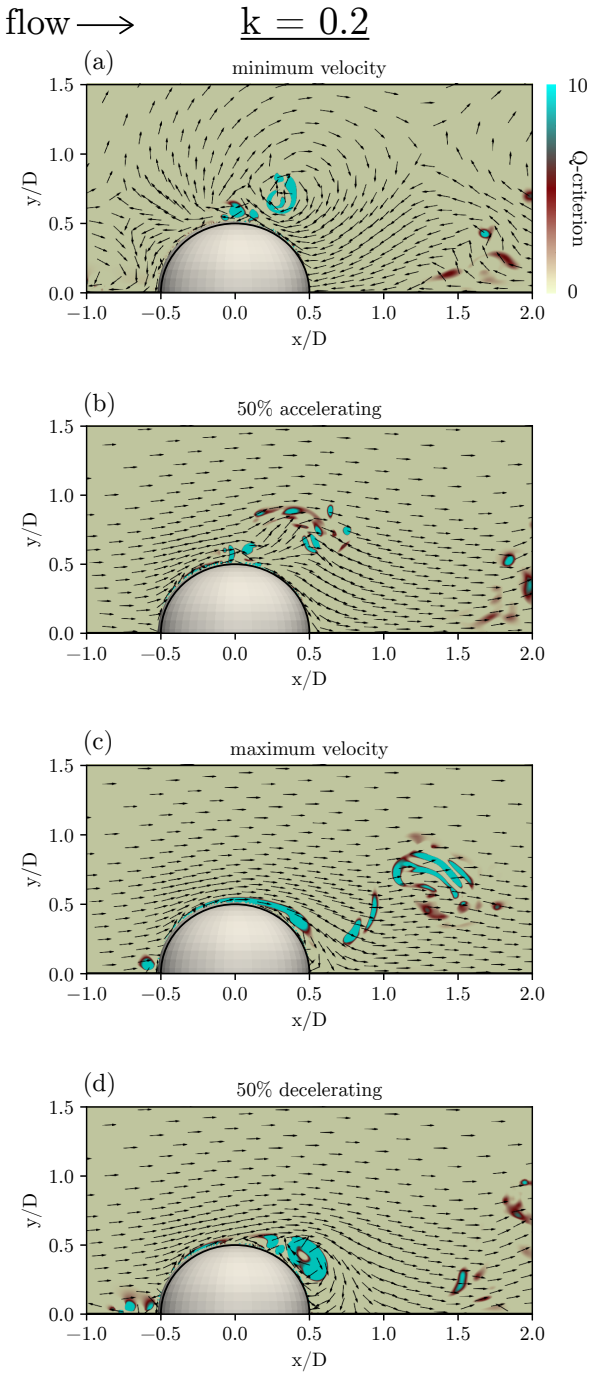

Figure 7. Velocity vector fields with Q-criterion contours around a surface-mounted hemisphere in highly pulsatile flow for the $k = 0.2$ case.

wake is entirely transformed from the quasi-steady case and is now dominated by the freestream pulsatility. The wake is now composed of an smooth arch-type structure which forms, propagates upstream, and is convected downstream all while retaining relative coherence. When compared to the original flow field, or a steady flow field, the wake topology is entirely changed. Starting with minimum velocity, Fig. 7(a), a series of relatively compact vortex structures can be observed near the crest of the hemisphere ($x/D = -0.1 to 0.5$, $y/D = 0.7$. The downstream-most and largest of these structures is the arch vortex. The three vortex structures upstream of the arch vortex are secondary vortices produced by the interaction between the arch and the solid surface of the hemisphere, similar to the phenomenon associated with vortex rings (Walker *et al.*, 1987). As the freestream accelerates, these structures are exposed increasingly intense shear which is likely the primary contributor to their loss of coherence in Fig. 7(b) and (c). In Fig. 7(c) the separated Q-criterion region on the leeward side of the hemisphere has a concentration at its downstream most extent. This concentration grows, as the freestream decelerates, to form the contained, singular arch vortex in Fig. 7(d). Additionally, due to the temporal compression of a period at high k, the remnants of the arch-type vortex from the previous cycle travel only a few D downstream remaining observable at $x/D \approx 2$ at 50% decelerating inflow (Fig. 7(d)).

DISCUSSION

The contour maps of Q-criterion in Figs. 4, 5, 6, and 7 are slices which serves as a representation of the more complex structure. Using three-dimensional representation of Q-criterion allows us to appreciate the structure fully.[1] Figure 8 is a series of isosurface of Q-criterion representation of the arch vortex in the $k = 0.2$ case. This, when coupled with the contours in Fig. 7, provides a full picture of the transformed wake of the hemisphere in pulsatile flow.

Using these results it is possible to produce a regime map of hemisphere wakes in pulsatile flows through reduced frequencies. Figure 9 is a series of schematic depictions of the wake regimes observed through changing k. This map ranges from the quasi-steady regime to the pulsatility-dominated wake topology. While course, only representing four values spanning an order of magnitude, the primary morphological changes of the wake are captured.

Starting from the low-frequency end of the span studied, the wake features closely resemble that of a steady flow — a turbulent mixing region in the near wake and hairpin vortices shedding from the shear layer's downstream-most extent. In the next regime the turbulent, near-wake mixing is observed, but the hairpin formation is suppressed. Moving higher in k, in the range of $k = 0.1$, the near wake appears organized into a single structure, aldthough the boundaries are not clearly defined. This structure, while arch-like in morphology, is not a single, smooth structure and is thus termed ragged. Finally, around $k = 0.2$ the wake is complete replaced with a single, smooth arch-type vortex. A map such as this may prove useful for researchers studying wakes and pulsatile flows in the future.

CONCLUSION

The effects of the frequency of freestream pulsatility on the flow surface-mounted hemisphere has been investigated. From the computed values, a set of four values of k have been presented. On one end of the range of k is $k = 0.01$ low frequency pulsatility producing a set of flow fields which are topologically similar to the flow structures in steady flow. At $k = 0.05$ the hairpin vortex shedding from the shear layer is no longer observed. At $k = 0.1$ a ragged arch-type vortex is observed in the near wake. At $k = 0.2$

[1]The contour maps in Figs. 4 5, 6, and 7 were used to avoid selecting a value of Q-criterion which adds a level of subjectivity and is required for the use of isosurfaces. The primary results were presented in this fashion to give as objective a representation as possible using a vortex identification method.

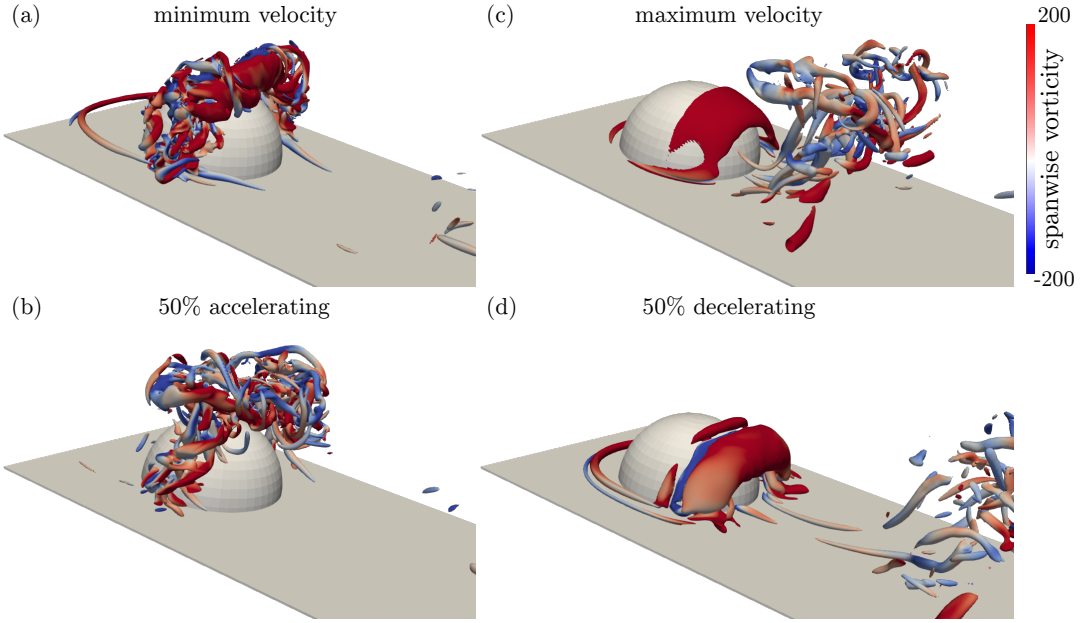

Figure 8. Isocontours of three-dimensional Q-criterion (Q = 15) colored by spanwise vorticity

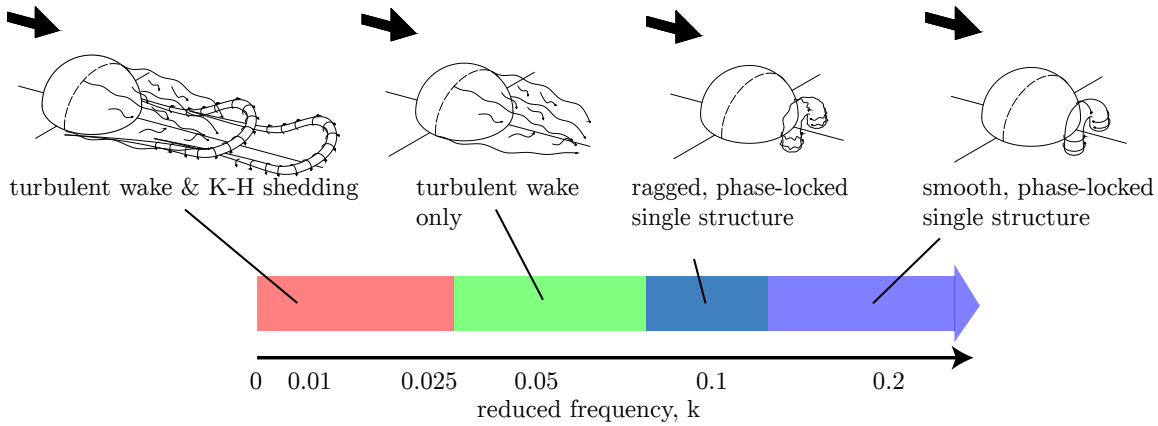

Figure 9. A map of wake regimes and associated coherent structures in the wake.

the arch-type vortex is clearer and more compact. A map of these regimes has been presented. The possible parameter space of a pulsatile flow is large. While this study focuses on the effects of pulsation frequency, the range of frequencies and canonical nature of the geometry provides a useful reference for engineers and researchers studying complex, application specific pulsatile flows.

REFERENCES

Acarlar, M. S. & Smith, C. R. 1987 A study of hairpin vortices in a laminar boundary layer. Part 2. Hairpin vortices generated by fluid injection. *Journal of Fluid Mechanics* **175**, 43.

Beratlis, N., Balaras, E. & Kiger, K. 2007 Direct numerical simulations of transitional pulsatile flow through a constriction. *Journal of Fluid Mechanics* **587**, 425–451.

Carr, Ian A. & Plesniak, Michael W. 2016 Three-dimensional flow separation over a surface-mounted hemisphere in pulsatile flow. *Experiments in Fluids* **57** (1), 1–9.

Hunt, J C R, Wray, A A & Moin, P 1988 Eddies, streams, and convergence zones in turbulent flows. In *Studying Turbulence Using Numerical Simulation Databases, 2. Proceedings of the 1988 Summer Program*, , vol. 1, pp. 193–208.

Walker, J. D. a., Smith, C. R., Cerra, a. W. & Doligalski, T. L. 1987 The impact of a vortex ring on a wall. *Journal of Fluid Mechanics* **41** (5), 99–140.